

Experimental and analytical behaviour of cogged bars within concrete filled circular tubes

Tilak Pokharel^{*1}, Huang Yao^{1a}, Helen M. Goldsworthy^{1b} and Emad F. Gad^{2c}

¹ Infrastructure Department, University of Melbourne, Parkville, VIC 3010, Australia

² Faculty of Science, Engineering and Technology, Swinburne University of Technology, Hawthorn, VIC 3122, Australia

(Received October 22, 2014, Revised November 24, 2015, Accepted January 05, 2016)

Abstract. Recent research on steel moment-resisting connection between steel beams and concrete filled steel tubes has shown that there are considerable advantages to be obtained by anchoring the connection to the concrete infill within the tube using anchors in blind bolts. In the research reported here, extensive experimental tests and numerical analyses have been performed to study the anchorage behaviour of cogged deformed reinforcing bars within concrete filled circular steel tubes. This data is essential knowledge for the design of the steel connections that use anchored blind bolts, both for strength and stiffness. A series of pull-out tests were conducted using steel tubes with different diameter to thickness ratios under monotonic and cyclic loading. Both hoop strains and longitudinal strains in the tubes were measured together with applied load and slip. Various lead-in lengths before the bend and length of tailed extension after the bend were examined. These dimensions were limited by the dimensions of the steel tube and did not meet the requirements for “standard” cogs as specified in concrete standards such as AS 3600 and ACI 318. Nevertheless, all of the tested specimens failed by bar fracture outside the steel tubes. A comprehensive 3D Finite Element model was developed to simulate the pull-out tests. The FE model took into account material nonlinearities, deformations in reinforcing bars and interactions between different surfaces. The FE results were found to be in good agreement with experimental results. This model was then used to conduct parametric studies to investigate the influence of the confinement provided by the steel tube on the infilled concrete.

Keywords: anchorage; cogged bar; blind-bolt; concrete filled steel tube; finite element analysis

1. Introduction

In the past few decades the anchorage behaviour of reinforcing bars in conventional reinforced concrete structures has been studied extensively. The bond behaviour between deformed reinforcing bars and the surrounding concrete has been investigated by pull-out tests on both short straight segments of rebar embedded in concrete (Eligehausen *et al.* 1983, Soroushian and Choi 1989, Soroushian *et al.* 1991, Hossain and Khandaker 2008, Kamal *et al.* 2013) and long straight specimens of rebar anchored in concrete (Scott 1996, Plizzari *et al.* 1998, Seo *et al.* 2014). Tests

*Corresponding author, Ph.D. Student, E-mail: tilakp@student.unimelb.edu.au

^a Ph.D., E-mail: jackyao@unimelb.edu.au

^b Associate Professor, E-mail: helenmg@unimelb.edu.au

^c Professor, E-mail: egad@swin.edu.au

have also been conducted to examine the behaviour of beam reinforcement anchored by 90-degree standard hooks inside reinforced concrete columns (Soroushian *et al.* 1988, Kang *et al.* 2010). However, research investigating the anchorage behaviour of straight or cogged reinforcing bars in concrete-filled circular steel tubes is very limited. The objectives of this study were to evaluate the adequacy of the anchorage capacity of the cogged bars, to determine the effect of confinement level on the load-slip behaviour and hence to evaluate the stiffness, and to investigate the effect of cyclic loading on deterioration of bond and anchorage. Recent research on steel moment-resisting connection between steel beams and concrete filled steel tubes has shown that there are considerable advantages to be obtained by anchoring the connection to the concrete infill within the tube using anchors in blind bolts (Yao *et al.* 2008). Other researchers have used the similar concept of embedding blind bolts into the concrete (Tizani *et al.* 2013, Pitrakkos and Tizani 2013). Because of space limitations in the tube, cogged bar anchors with a shorter lead-in length than that required in typical standards have been included in the study. This paper presents result from a series of pull-out tests on anchored bars. In addition, results from a non-linear 3D finite element analysis are presented and compared with test results. This model was then used to conduct parametric studies to investigate the confinement provided by the steel tube on the infilled concrete.

2. Experimental program

2.1 Test specimens

The pull-out specimens were tested under either monotonic or unidirectional cyclic loading to study the load-slip behaviour of cogged and straight reinforcing bars anchored in concrete-filled steel tubes. The basic specimen is shown in Fig. 1. It consisted of a one metre long circular hollow section produced in accordance with AS1163 (1991) (Diameter 323.9 mm with thickness of 6, 8, and 10 mm) filled with normal strength concrete. The grade of the steel tube is C350L0. Reinforcing bars complying with AS/NZS 4671 (2001) of 16 mm diameter and N-type (deformed ribbed bars of grade 500 MPa normal ductility steel), either straight or cogged, were anchored within it. The characteristic compressive strength of the concrete infill was designated to be 45 MPa. The mean compressive strength of the test specimens were 47.5 MPa with a standard deviation of 1.2 MPa. Different cogs were dimensioned in accordance with the requirements of either AS3600 (2001), Eurocode 2 (CEN 2004), and ACI (2005) respectively. Coupon tension tests were performed on the reinforcing bars and the results are presented in Table 1. In this table, nominal properties of the circular tube material are also given.

The tests were composed of five series, with eight groups in total. A list of the specimens in each group indicating cogged bar type, bar size, concrete strength, embedment length, and loading type is provided in Table 2. The first series had three testing groups: Groups G1A, G1B, and G1C. It involved testing specimens with a standard AS3600 (2001)-type cog and with a straight lead-in length. The second series consisted of two testing groups, Groups G2A and G2C. The specimens in this series had a shortened cog dimensioned in accordance with the Eurocode 2 (CEN 2004) with a reduced straight length. The third series had one group, Group G3A, in which the specimens had a pure cog without any lead-in portion. The fourth series, Group G4A, involved tests on a straight reinforcing bar, and a fifth series, Group G5A, involved testing a cog for which the geometry of the bend follows the ACI requirement (ACI 2005).

Table 1 Material properties

Test coupon	Yield stress (MPa)	Tensile strength (MPa)	Ratio (tensile strength/yield stress)	Uniform elongation (%)
Reinforcing bar	541	636	1.17	8.6
Circular tube	350	448	1.28	14.0

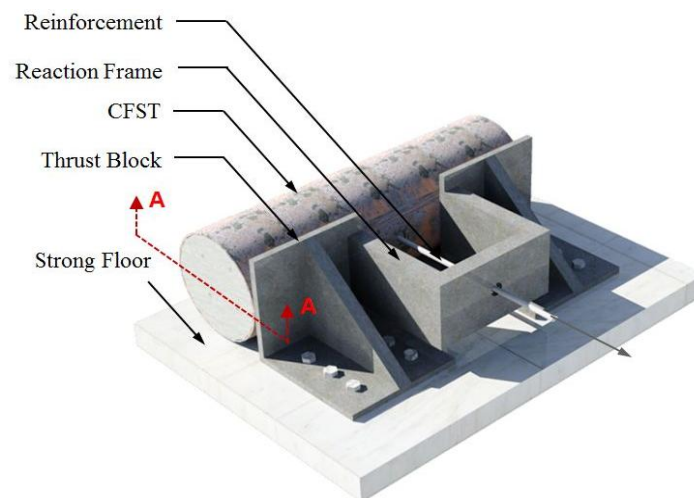


Fig. 1 Isometric view of pull-out test specimen

Specimens in Groups G1A, G2A, G3A, G4A, and G5A were subject to monotonic loading, whereas specimens in Group G1B were subject to cyclic loading of Type I, and specimens in Groups G1C and G2C were subject to cyclic loading Type II. Loading Type I is made up of 20 load cycles at 60 kN and 10 load cycles at the yield plateau. In loading Type II, the number of load cycles applied was doubled at each load stage compared with those in Type I.

The pull-out tests in Groups G1A, G2A, and G3A were designed to evaluate the adequacy of the anchorage behaviour of cogged bars within steel tubes of varying diameter to thickness (D/t) ratios. These monotonic tests were useful in determining the effect of confinement level on the load versus slip behaviour of the embedded bars. The cyclic loading tests for Groups G1B, G1C, and G2C were designed to investigate the deterioration of bond and anchorage under a number of loading cycles at two different load levels. Group G4A covered testing of straight bars embedded in 6 mm thick tubes (D/t ratio of 54). Group G5A involved testing cogged bars bent in accordance with the ACI requirements and embedded in 6 mm thick tubes (D/t ratio of 54).

2.2 Test setup and instrumentation

The pull-out tests were set up as depicted in Fig. 1. The concrete-filled steel tube was laid against two thrust blocks bolted to the structural floor. The cogged bar was anchored in the tube and then passed through the reaction frame and was fixed into a gripping mechanism. The tests were run under a monotonic displacement-controlled force arrangement using a hydraulic jack with a displacement rate of approximately 1mm/minute.

The instrumentation shown in Fig. 2 was used to measure bar slip from the tube, strain in the bar and strain in the tube wall. Four LVDTs were mounted on a lateral support to measure the relative displacements at a predefined distance from the surface of the tube. The needles of transducers T1 and T4 were set on the tube wall, whereas those of transducers T2 and T3 were set on a reference ring that was secured to the bar at the entrance of the bar to the tube. The measured displacement of T1 and T4 resulted from two superimposed factors: (1) the elongation of the rebar itself over the predefined length outside the tube recorded by T2 and T3; and (2) the slip of the cogged bar with respect to the surrounding concrete in the tube. Hence, the slip value was calculated as

$$\delta_{slip} = \delta_{total} - \delta_{bar}$$

Where,

- δ_{slip} = Slip of cogged bar in the concrete-filled steel tube;
- δ_{total} = Average displacement measured by T1 and T4; and
- δ_{bar} = Stretching of bar over the thickness of the tube wall and the predefined length outside of tube (adjusted by the average displacement measured by T2 and T3).

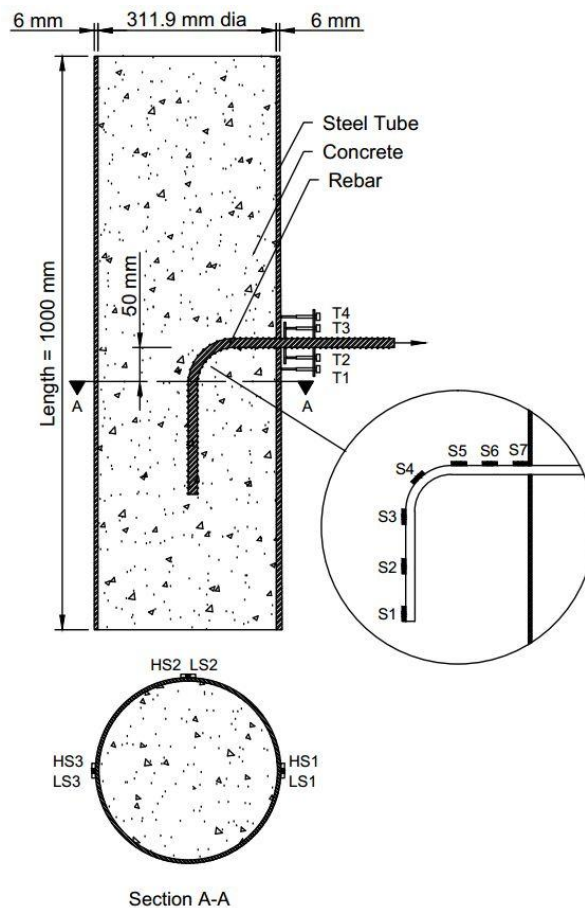


Fig. 2 Instrumentation of pull-out test. Here, S represents strain gauge on rebar, HS and LS represent strain gauge on tube for hoop and longitudinal strain respectively and T represents LVDT

To monitor the strain of the steel tube for each specimen, six strain gauges (LS1, LS2, LS3, HS1, HS2, and HS3) were mounted on the outer face of the tube in the longitudinal and transverse directions at three positions. The first position was 50 mm away from the bar measured along the tube in the direction of the cog, the second position was 90 degree counter clockwise from the first location at the same cross-section, and the third position was on the opposite side to the first location. In the series of tests involving monotonic loading, strain variation along the cogged bar within the concrete was also measured by seven strain gauges (S1, S2, S3, S4, S5, S6, and S7) protected with epoxy resin and spaced at intervals along the bar.

3. Experimental results

3.1 Observed failure mode

The equivalent straight development length provided by the combined cog and straight length of the bar within the tube is 271 mm for Groups G1A & G1B & G1C, 173 mm for Groups G2A & G2C, 220 mm for Groups G3A, 324 mm for Group G4A, and 379 mm for Group G5A. All of these are less than the development length of 400 mm required by the Australian Concrete Structures Standard AS3600 and of 574 mm required by the ACI code. Despite this, in all of the cogged bar anchorage tests, failure was caused by breaking of the bar outside the steel tube. None of the bars was pulled out from the tube due to an anchorage failure. The cogged bars all experienced yield and then reached their ultimate strength. In conventional concrete structures, splitting of concrete cover in the plane of the cog is the primary cause of failure of cogged bars, and that splitting originates at the inside of the cog where the local stress concentration is very high. In the concrete-filled steel tubes, the splitting of the concrete cover is inhibited by the surrounding steel tube encasement.

3.2 Slip of the bar

Tension load versus slip is a key relationship in the pull-out tests. Figs. 3 to 6 show the load versus slip response under monotonic loading conditions for specimens within Groups G1A, G2A, G3A, G4A and G5A respectively. The reported results are for the average of two test specimens. In the proposed blind-bolted connection being examined, the force in the bolt extension (and hence the cogged bar tested here) would be limited to approximately 60 kN (60% of ultimate bar capacity), even under a severe earthquake. This would be achieved during the design by creating a certain strength hierarchy between the members and connection components. At 60 kN, slip values of 0.45 mm, 0.39 mm, 0.33 mm took place for specimen G1A_t6, G1A_t8, and G1A_t10 respectively. These slip values were predominantly due to elongation of the bars within the concrete. As the load increased, a certain degree of bond loss occurred along the straight length of the bar, as discussed in more detail in Section 3.4, leading to a greater reliance on the compression strut generated in the concrete by bearing stresses from the cog. At the bar's yield load of 105 kN, accumulated slips of 1.13 mm, 0.97 mm and 0.78 mm respectively were obtained for specimens G1A_t6, G1A_t8 and G1A_t10. As sufficient length of the vertical portion following the bend was provided, full strength of the cogged bar was achieved.

The specimens in Group G2A have their lead-in lengths and cog tail lengths halved compared to those specimens in Group G1A. As a result of reduced length before and after the bend, the cogged bars in Group G2A tended to slip more than G1A as the load increased. In Group G3A, the

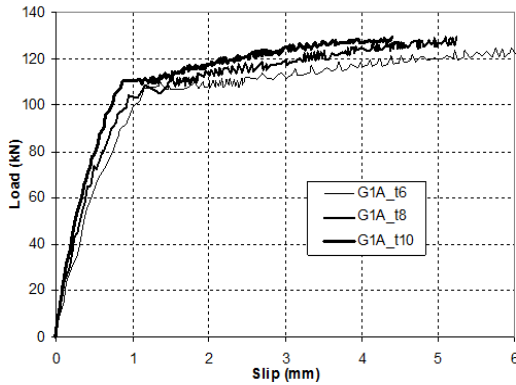


Fig. 3 Load-slip of Group G1A

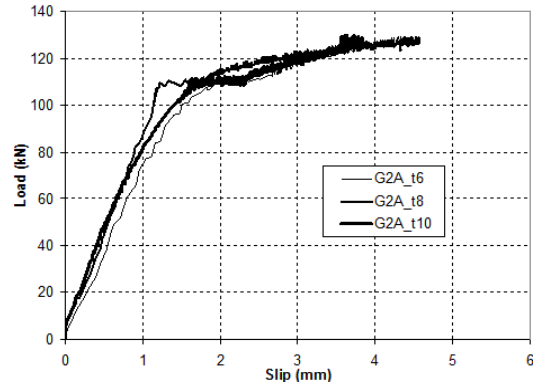


Fig. 4 Load-slip of Group G2A

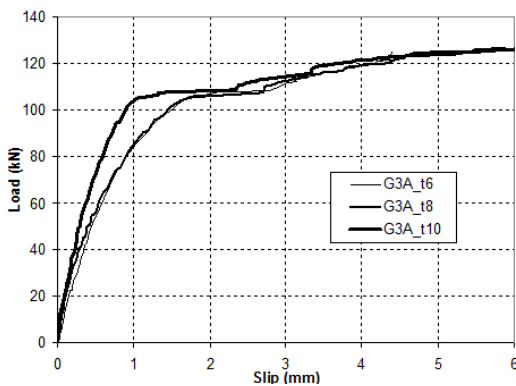


Fig. 5 Load-slip of Group G3A

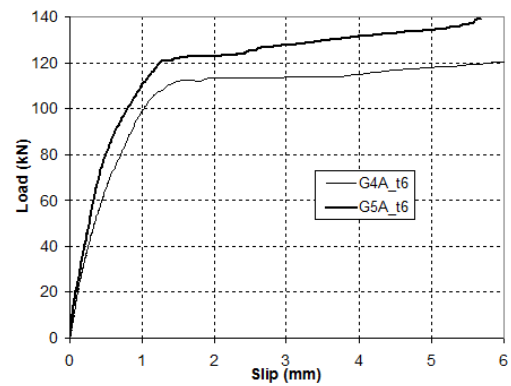


Fig. 6 Load-slip of Groups G4A & G5A

straight lead-in portion was debonded; the anchorage was thus provided by the cog with an identical geometry to that of specimens from Group 1A. Therefore, the cogged bars in Group G3A were more flexible than those in Group G1A, but stiffer than specimens in Group G2A. The detailed slip values at load levels of 60 kN and 105 kN are listed in Table 3. Comparisons of slip values provide a deeper understanding of the anchorage behaviour of the cogged bars.

The Group G4A involved tests of straight bars embedded in steel tubes of 6 mm thickness with the same length as the internal diameter of the tubes and Group G5A involved tests of cogged bars bent in compliance with the ACI requirement in the corresponding size of tubes. As indicated in Fig. 7, G4A_t6 has a comparable anchorage performance to that of G1A_t6. In other words, the cogged bar formed in accordance with AS3600 requirement with a short lead-in length is equivalent to straight bars anchored across the whole section of the steel tubes. G5A_t6 achieved superior anchorage behaviour compared to the other types of embedded bars as the ACI requirement was for a greater lead-in length, bend radius, and cog tail length. It was stiffer in the elastic region. The slope of its plastic section was about the same as for the others.

3.3 Cyclic behaviour

A detailed investigation was conducted to determine the robustness of the anchorage when

Table 3 Slip of cogged bar

Load	Slip (mm)										
	G1A			G2A			G3A			G4A	G5A
	t6	t8	t10	t6	t8	t10	t6	t8	t10	t6	t6
60 kN	0.45	0.39	0.33	0.79	0.66	0.66	0.59	0.54	0.37	0.45	0.33
105 kN	1.13	0.97	0.78	1.74	1.54	1.18	1.68	1.71	1.03	1.14	0.89

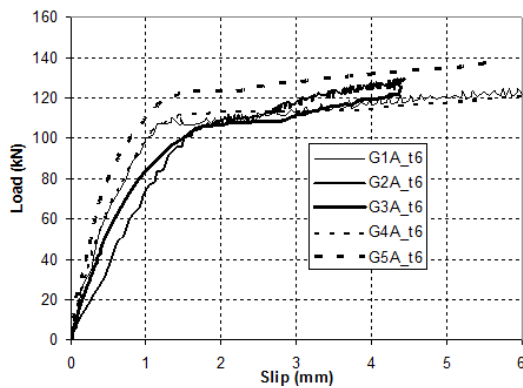


Fig. 7 Load-slip of various cog types anchored in 6 mm tubes

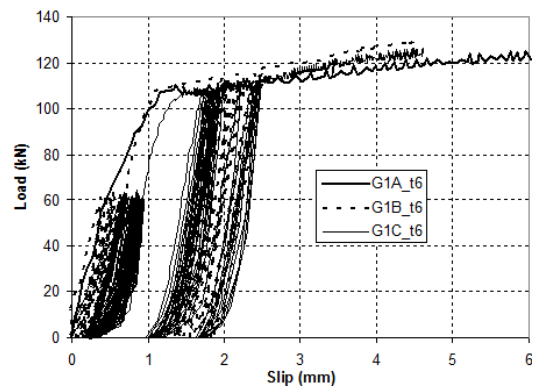


Fig. 8 G1B_t6 & G1C_t6 under cyclic loading

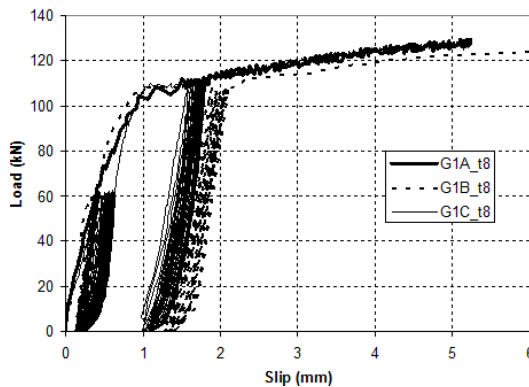


Fig. 9 G1B_t8 & G1C_t8 under cyclic loading

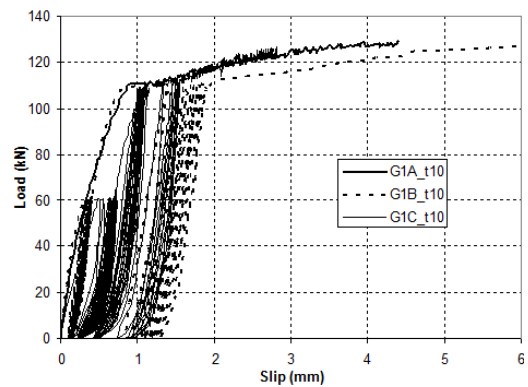


Fig. 10 G1B_t10 & G1C_t10 under cyclic loading

subjected to cyclic loading. This could be important in connections such as those in Yao (Yao *et al.* 2008) when a very rare earthquake event is experienced by the frame. As discussed Section 3.2, the tensile force in the bolt extension would be limited to 60% of bolt capacity which is 60 kN; so the behaviour of the extension when loaded from 0 kN to 60 kN and back to 0 kN for several cycles is of interest. Specimens in Group G1B were subjected to 20 cycles at 60 kN and 10 cycles at a load just above the yield level (Type I loading). More cycles were applied to specimens in Groups G1C and G2C; namely, 40 cycles at 60 kN and 20 cycles just above the yield load (Type II loading). While this number of cycles is excessive when compared with the expected number of cycles for a design earthquake, all of the cogged bars performed well when subjected to cyclic

loading in the two series of pull-out tests. This indicates a very high level of robustness for this form of anchorage within circular steel tubes.

Figs. 8 to 10 show the load versus slip response of specimens in Groups G1B and G1C under cyclic loading Type I and Type II. In these figures, the force-slip behaviour for cogged bars tested monotonically is superimposed on the curves of force-slip tested cyclically. When cycling at 60 kN there is a small increase in the slip for each cycle of loading, indicating some deterioration in the bond (this is discussed further in Section 4.4). Superimposing these curves show that the cyclic backbone load-slip curves are similar to the corresponding monotonic load-slip curves.

3.4 Strain distribution along the bar

A typical strain distribution along the cogged bar within the concrete-filled steel tube is shown in Fig. 11 for the specimen G1A_t6. The locations of strain gauges S1 to S7 are given in Fig. 2. Due to bond between the concrete and the bar, the strain in the bar gradually decreased with distance from the hole in the tube wall. The difference in strain between S7 and S5 indicates that bond was effective along the straight length of the cog in these monotonic tests. However, after the steel strain exceeds the yield strain within the short lead-in length of the bar there is little

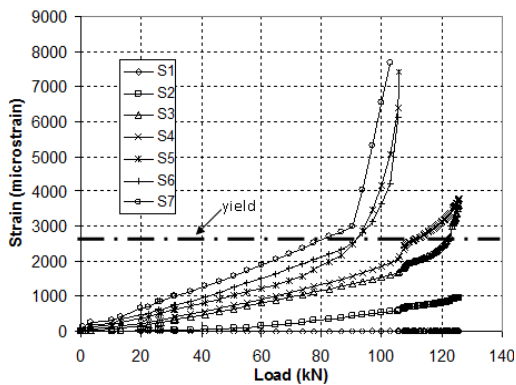


Fig. 11 Strain on cogged bar of G1A_t6

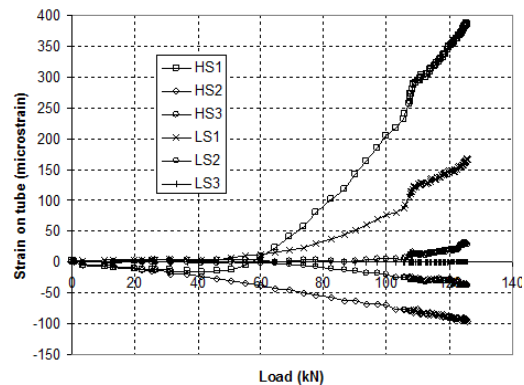


Fig. 12 Hoop strain and longitudinal strain vs. load for specimen G1A_t6

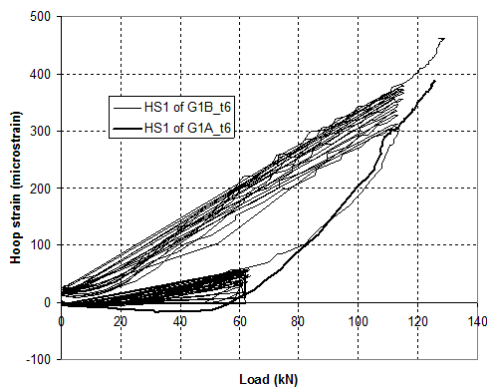


Fig. 13 Comparison of hoop strains in specimen G1A_t6 and G1B_t6

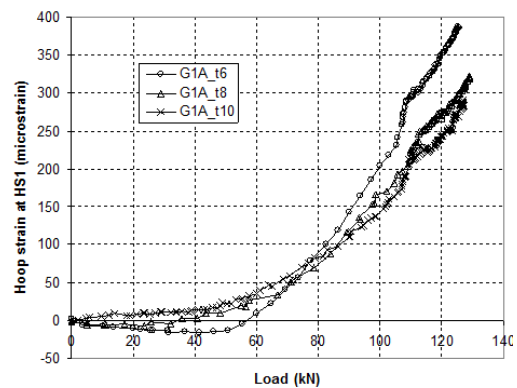


Fig. 14 Hoop strain at HS1 for specimens in group G1A

difference between the strain in S7 and S5 and reliance is then placed entirely on the cog and the cog tail to resist the bar pull-out. This is because once the rebar yields, the bond stress will be decreased either by local crushing of concrete under the ribs.

3.5 Strain on the tube wall

Under a load of 60 kN, the hoop strains at HS1, HS2 and HS3 in the tube were less than 50 microstrain in the transverse direction as the concrete itself could restrain the bar and sustain the applied load with little lateral expansion. As the load increased, the compressive force applied by the cog onto the concrete caused the concrete to expand and bear on the tube wall. Therefore, some transverse strain was then recorded in the tube wall. As expected, more strain was recorded in the thinner tube (6 mm) compared to the thicker tubes. Fig. 12 shows the hoop strains and longitudinal strains recorded in specimen G1A_t6. The longitudinal strains were nearly one-third of the corresponding transverse hoop strains. This is due primarily to the Poisson's effect. The strains remained low even at the ultimate load, with a maximum value of 400 micro-strains in the transverse direction. Fig. 13 compares the hoop strain of specimen G1B_t6 at HS1 under cyclic loading Type I with that of specimen G1A_t6 subject to monotonic loading. From Fig. 13 it is evident that there was a small increase in the hoop strain with each cycle of load suggesting that further localized micro-cracking of the concrete within the tube had occurred with each cycle. After the cyclic loading the hoop strain vs. load curve returned to the monotonic one. The comparisons of hoop strains at HS1 in the tubes of 6, 8, and 10 mm thickness are shown in Fig. 14.

4. Discussion of experimental results

4.1 Effect of straight portion

The accumulation of bond damage along the straight portion of the extension at load levels higher than 60 kN is caused by the progressive growth of micro-cracks and concrete micro-crushing in front of the protruding lugs. In test group G3A, the straight lead-in length of $3.2d_b$ was debonded and resistance to the tension load relied purely on the cog, whereas group G1A had a similar configuration, but with the straight lead-in length embedded in the concrete. Comparing the load versus slip of specimen G1A_t6 with that of specimen G3A_t6 shown in Fig. 7, it is found that the initial stiffness improved if the embedded lead-in portion were present. Otherwise, the overall response of the two specimens is similar indicating that the cog behaviour is dominant. It should be noted that under some loading situations the contribution of the straight lead-in portion to the anchorage would be partially discounted, for example due to tensile flexural cracks in the column under cyclic loading from a high level seismic event (Paulay and Priestley 1992).

4.2 Effect of cogged portion

Cogs play an important role in preventing the bar from pulling out of the concrete after the loss of bond along the straight lead-in length. A cog works by bearing as indicated by the difference in strains between S3, S4, and S5 at the bend as shown in Fig. 11. A comparison between specimen G5A_t6 and specimens G1A_t6 and G2A_t6 in Fig. 7 shows that the stiffness and capacity of a cogged bar increases with increased bend radius. The strain decreases rapidly from the start of the tail at S3 to the tip of the tail at S1 (where it is zero) as shown in Fig. 11. As the straight lead-in

length was relatively short, the bend portion played a substantial role in resisting the pull-out load. Thus a significant proportion of the tension load was carried by the cog.

4.3 Effect of confinement

The measure hoop strain on the tube wall provided an indication of confinement effects on the in-filled concrete. Assuming a strip at the measured spots with an identical unit height, the hoop strain could be converted into hoop stress in the tube wall. Thus, the radial confining pressure was determined by $p = \sigma_h t / r$, where t and r are thickness and internal radius of the tube. At the bar's yield load of 105 kN, the confining pressures of 1.86 MPa, 2.00 MPa, and 2.27 MPa were obtained for specimens G1A_t6, G1A_t8 and G1A_t10 respectively. Although there was a minor improvement to the load-slip behaviour by increasing the tube thickness from 6 mm to 10 mm as illustrated in Figs. 3, 4 and 5, it appears that at this load level the tube with 6 mm thickness ($D/t = 54$) was capable of providing a similar level of confinement to the in-filled concrete as the thickest tube ($D/t = 32$).

4.4 Effect of cyclic loading

Cyclic loading at moderate to high stress levels may introduce a progressive deterioration of bond in the anchored bar. Bond and anchorage resistance before failure is provided by bearing of the lugs on the concrete, thus concrete strength is a key parameter.

With respect to the performance of specimens G1B_t8 and G1C_t8 shown in Fig. 9, little deterioration of anchorage was observed at the load cycles at 60 kN. In the cyclic tests performed on specimen G1C_t8, the residual slip after 5 cycles at 60 kN was 0.08 mm. This is likely to be the maximum number of large cycles expected in an earthquake. Even if further 15 cycles were imposed, the total residual slip would be only 0.14 mm.

The performance of the bar due to cyclic straining at a selected position along the yield plateau is reported here, although it is not expected that this will be utilized in design. The accumulated slip occurring due to cycling at a selected position along the yield plateau was due mostly to the plastic elongation of the bar within the tube. In specimen G1C_t8, the residual slip after 5 cycles at 110 kN was 0.16 mm. The total residual slip was 0.22 mm after another 5 cycles.

5. Analytical modelling

5.1 FE model

Several models have been reported in the literature for the pull-out behaviour of reinforcement from concrete (Soroushian *et al.* 1988, Yao *et al.* 2008, Haskett *et al.* 2008). Bond between deformed reinforcement bars and concrete along the length of the bar is mainly due to the bearing of rebar lugs on the concrete i.e., the bond resistance is mainly due to the wedge force from the rebar lug acting around the surrounding concrete when the pull-out load is applied (Seo *et al.* 2014). The previous models do not explicitly consider the effect of bearing of lugs on the concrete. In this research, the pull-out behaviour of straight and cogged reinforcement bars is simulated by taking the lugs into consideration in a finite element simulation.

ABAQUS/Explicit was used for the analysis. Geometric nonlinearity, material nonlinearity and the interaction between different surfaces is considered in the analysis. The concrete elements in

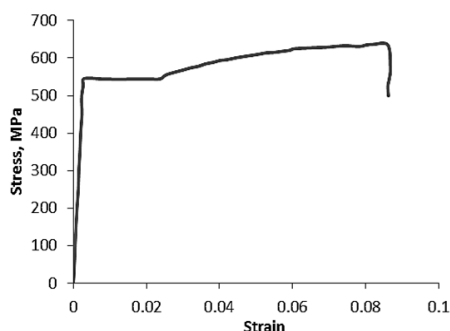


Fig. 15 Stress-strain relationship of N type bar

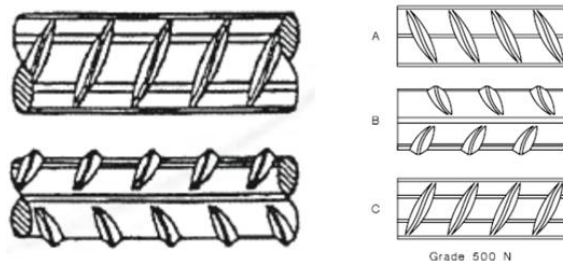


Fig. 16 Deformed pattern of N type reinforcing bar

this analysis were modelled using the nonlinear Concrete Damage Plasticity (CDP) model with linear stress-strain behaviour up to 40% of concrete stress (Mirza and Uy 2011). This model is versatile and capable of predicting the behaviour of concrete structures subjected to monotonic, cyclic and dynamic loading. “Tensile cracking” and “Compression Crushing” of the concrete are the two main failure mechanisms in CDP. The commencement of failure is controlled by compressive and tensile plastic strain (Abaqus 2012).

A nonlinear isotropic model was used to model the steel elements. The steel is normal ductility steel and the grade of steel is 500 MPa. Fig. 15 shows the result of a coupon tensile test of a reinforcement bar.

Surface to surface contact was used to simulate the interaction properties. Contact surfaces were allowed to separate from each other and the penetration of one surface to another was prevented. In all cases hard contact was used in the normal direction and frictionless contact was used in the tangential direction.

For this analysis, N type deformed reinforcement of 16 mm diameter was used, i.e., the same as in the experimental work. The pattern of deformation complies with Australian Standards AS/NZS 4671 as shown in Fig. 16.

The modelled circular steel tube was of the same material, diameter and length as that used in the tests, i.e., tube grade of C350L0, length of 1 m, and diameter of 323.9 mm are used. The wall thickness of the tube was chosen to be 6 mm in the simulation. The tube was filled with concrete with a mean compressive strength of 51 MPa.

5.1.1 Pull-out of Straight bar

The test set up for the pull out test has been shown in Fig. 1 and the embedment depth of rebar into the concrete is 312 mm which is nearly 19.5 times the diameter of the reinforcing bar. The lugs of the rebar have been approximated in the simulation as shown in Fig. 17 and the mid-section view (Section A-A of Fig. 1) is shown in Fig. 18.

One quarter of the actual model is modelled due to its symmetry in two axes. Fig. 19 shows the finite element representation of the test specimen. Symmetric boundary conditions were imposed on two symmetric planes, one longitudinal plane along the centre of the CFST and another transverse plane at middle of the CFST. A displacement controlled load is applied at the end of the reinforcement.

5.1.2 Pull-out of cogged bar

For the pull-out of a cogged bar, the same steel tube, concrete and reinforcement bar as

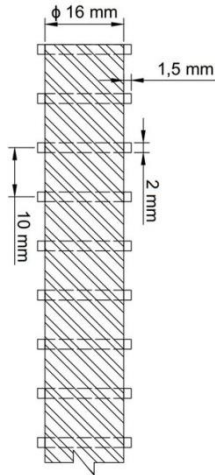


Fig. 17 Approximated deformed pattern of reinforcement bar

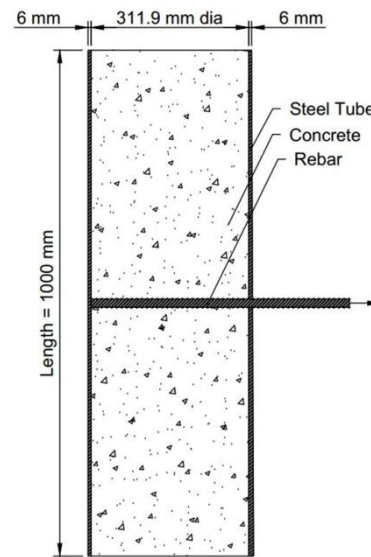


Fig. 18 Mid-section view of model (Section A-A of Fig. 1)

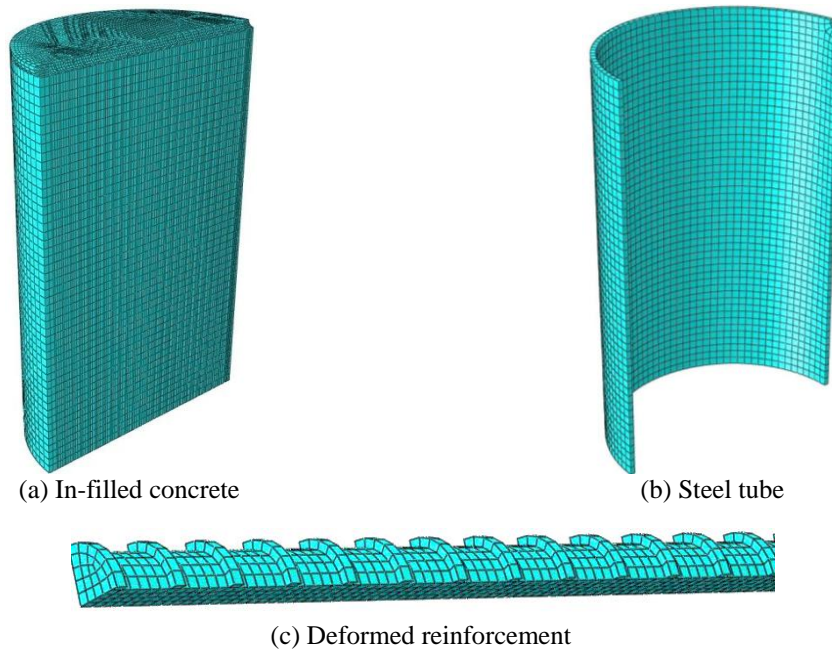


Fig. 19 Finite element mesh representation of pull out of rebar from concrete filled circular square tube. One quarter of the actual test is modelled

described in Section 5.1.1 were used. The lug arrangement was the same as that of the straight bar. The detailed geometry of the deformed reinforcement bar is shown in Fig. 22. The extension of the cogged bar is as per ACI requirements which is the same as Group G5A.

The simulation of the experimental set up was similar to the straight bar anchorage explained in Section 5.1.1. The mid-section view of the model is shown in Fig. 2.

The actual tested model was symmetrical about the vertical axis. Therefore, half of the model along the axis of symmetry is analysed. The FE representation is shown in Fig. 20. Displacement controlled load was applied to the end of the reinforcement in an outward direction. Since the majority of the bond along the length of the bar is due to the bearing of lugs in the reinforcement, the tangential friction between the rebar and concrete was neglected in this analysis.

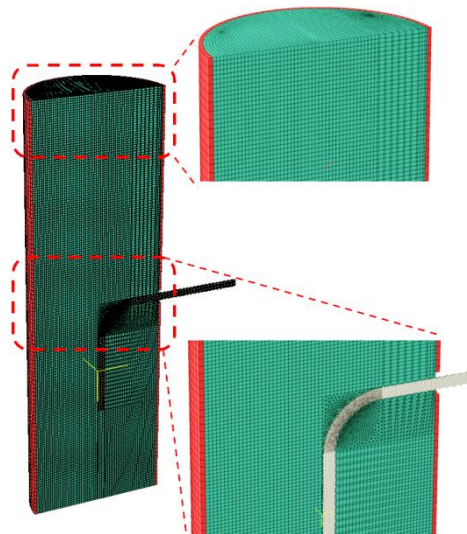


Fig. 20 Finite element representation of pull-out test of cogged anchored bar within concrete filled steel tubes. Due to the symmetry of the model, only the half of the actual specimen was modelled in the FE analysis. The red, green and grey colours in this figure represent the steel tube, in-filled concrete and deformed reinforcement bar respectively

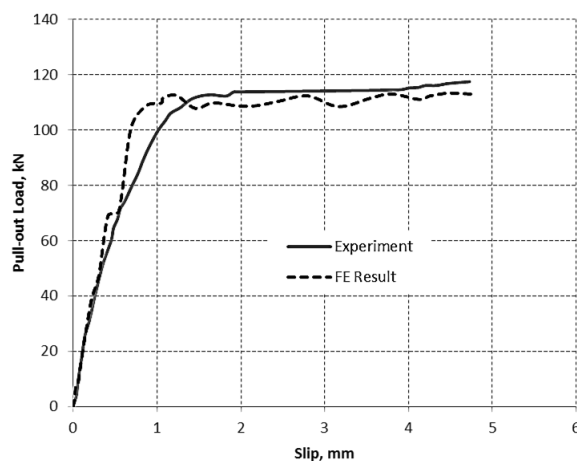


Fig. 21 Pull-out load vs. slip curves for pull-out of straight rebar from the concrete filled circular steel tube

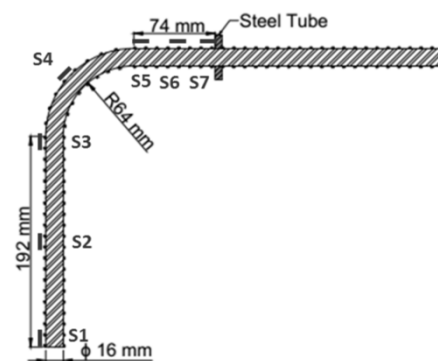


Fig. 22 Geometry of cogged reinforcing bar along with the location of strain gauges

As described in Section 3.2, for the connections proposed by Yao *et al.* (2008), the force in the bolt extension would be limited to 60% of its capacity. Therefore, the focus of this analysis is to check the stiffness of the connections up to this limit. Nevertheless, in order to provide further information for comparison with the experimental work, the analysis was not terminated until the rebar yielded. To verify the failure mode the complete behaviour up to failure was analysed for one case and the analysis successfully predicted the failure mode observed in the experiment, i.e., fracture of the reinforcement.

5.2 Analytical results

Fig. 21 shows the comparison of pull-out load vs. slip curves from the FE results and from the experiment for pull-out of a straight bar in Group G4A. There is a good agreement in both stiffness and ultimate load between the FE and experimental results. Failure occurred due to fracture of the reinforcement bar in both the experiment and the FE simulation.

Figs. 23 and 24 show the tension and compression damage of concrete at 60% of the rebar capacity and at the rebar failure condition respectively. Those figures represent the tensile cracking and the compression crushing of the concrete. The progressive bearing of lugs on surrounding concrete can be seen in the figures. Tensile cracking commences near the pulled end and there is still intact concrete at the other end. The concrete is crushed under the head of lug near the active end with no crushing at the other end. Eventually the stress at the active end reaches the ultimate tensile strength and the bar fractures.

Fig. 25 shows the pull-out load vs. slip curves for the cogged reinforcement (Group G5A). There is a good agreement between the experimental and the FE results. The slight difference could be due to variation in material properties from the tested sample, tangential friction between rebar and concrete (which is neglected in the analysis as explained earlier) or other approximations.

To see the effect of confinement provided by the steel tube the analysis was performed for

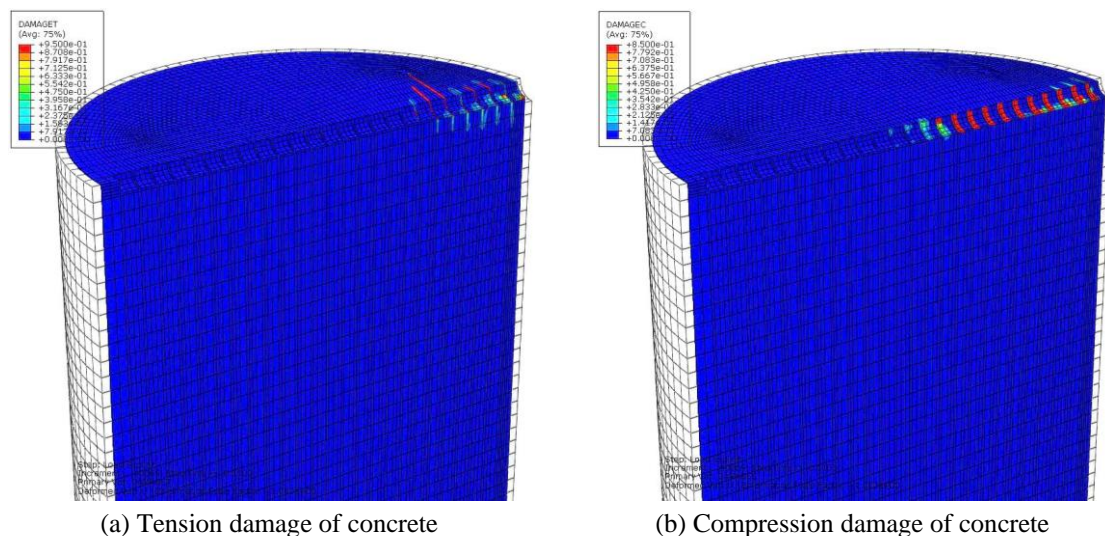


Fig. 23 Damage of concrete in tension and compression which is the representation of cracking and crushing of concrete respectively when the load at the bar is 60% of its capacity

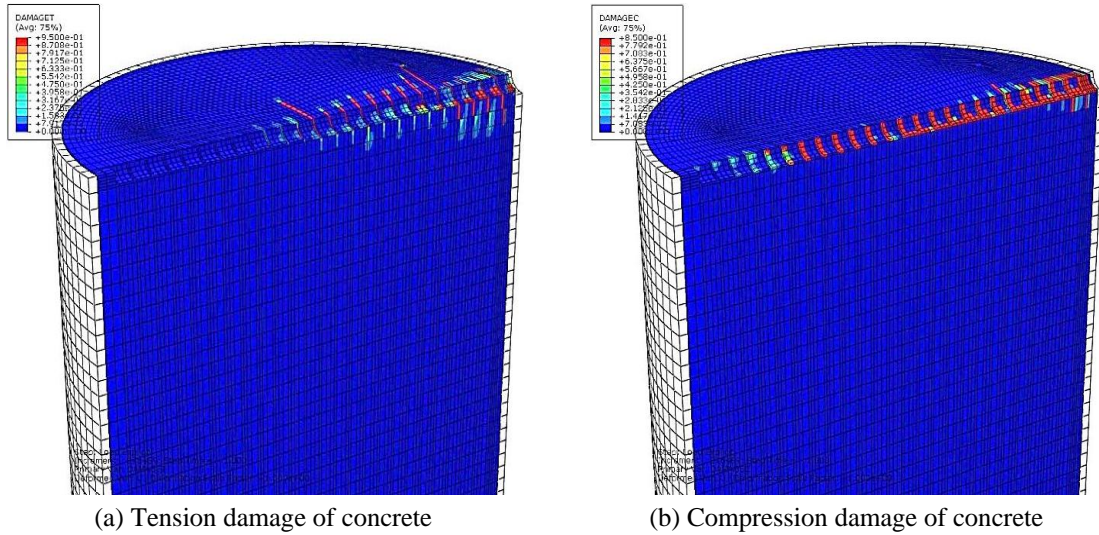


Fig. 24 Damage of concrete in tension and compression which is the representation of cracking and crushing of concrete respectively at rebar failure

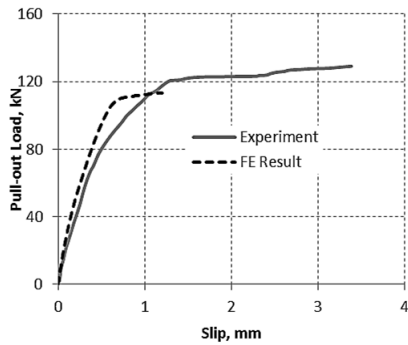


Fig. 25 Pull-out load vs. slip curves for pull-out of cogged anchored rebar from the concrete filled circular steel tube

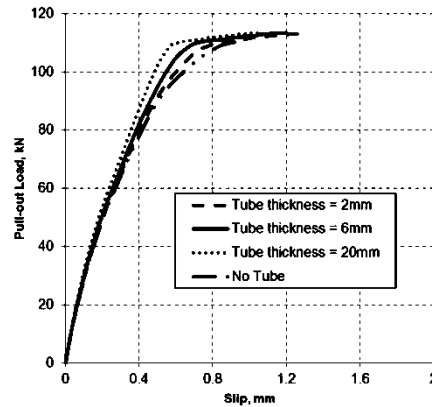


Fig. 26 Pull-out load vs. slip for pull-out of cogged anchored rebar from the concrete filled circular steel tube for different thickness of tube wall

different wall thicknesses. Fig. 26 shows the pull-out load vs. slip curves with no tube and for tubes with 2 mm, 6 mm and 20 mm wall thickness respectively. There is a very small variation in the stiffness and almost no change in the maximum load reached. This is because of the effectiveness of the surrounding concrete which is sufficient to prevent pull through of the reinforcement and to provide stiff behaviour. In the discussion of the effect of confinement on the experimental results in Section 4.3 small levels of confinement were shown to develop in the Group 1A specimens, with slightly higher values with increasing tube wall thickness at the point when yield was reached. These are likely to be due to expansion due to small micro-cracks formed due to bearing of the lugs on the concrete, and also the effect of the compression strut from the cog.

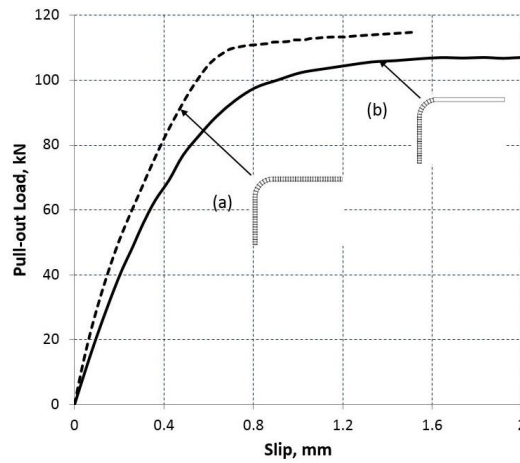


Fig. 27 Pull-out load vs. displacement for pull-out of cogged anchored rebar from the concrete filled circular steel tube with and without bond in straight lead-in length

A small effect due to confinement was found in the numerical results at the yield load, but very little at 60 kN as shown in Fig. 26. Also, the stiffness (secant value at 60 kN) calculated using the FE model matches well with the experimental work. There would be a greater effect of confinement (wall thickness) if the bar was bigger or there was a group of closely spaced bars, since in these cases it is likely that considerable pressure would be applied to the tube wall as a result of compressive struts emanating from the cog/s.

Fig. 27 shows the pull-out load vs. displacement curve of cogged bars for two cases: (a) considering bond between rebar and surrounding concrete along its length; and (b) debonding the initial straight length of rebar. In the second case, lugs were not modelled in the straight lead-in length. The stiffness of curve (b) is slightly less than that of curve (a). Similar trends were observed in the experiment, as shown in Fig. 7 where the slope of the pull-out load vs. slip curve for G3A is flatter than that of Group G1A. In terms of the values of the secant stiffness at 60 kN these are similar to the experimental results, with the FEA giving slightly stiffer results. As explained previously in Section 3, the initial lead-in length of the cog in Group G1A is de-bonded in Group G3A, but the specimens are identical otherwise.

6. Conclusions

Based on experimental studies and the FE analysis reported in this paper, the following conclusions can be drawn:

- The experimental studies and numerical analyses presented in this paper provide valuable information on the anchorage mechanism of cogged deformed bars used as anchors in concrete filled steel tubes. This knowledge is essential in determining the strength and stiffness of steel moment-resisting connections that use blind bolts with cogged anchors.
- A series of pull-out tests clearly demonstrate the ability of cogged bars within concrete-filled circular steel tubes to provide anchorage sufficient to develop the full strength of the bars. This is true despite the cogged bars having development lengths less than that required

in typical concrete structures standards such as AS3600 and ACI318, and shorter cog tails. In all of the cogged bar anchorage tests, failure was caused by breaking of the bar outside the steel tube. None of the bars was pulled out from the tube due to an anchorage failure.

- The diameter to thickness ratio of the steel tubes used in the experiment i.e., 32 to 54, has not been shown to have a significant influence on the monotonic load versus slip behaviour. The measured hoop strain on the tube wall provided an indication of a small confinement effect on the in-filled concrete at yield load in the bar, but very little at 60 kN load which is the maximum load in the anchor that could be allowed in the design of the composite connections. By examining the radial confining pressure for tubes, it was found that the effect imposed on the anchorage behaviour was marginal as the thinnest tube wall ($D/t = 54$) could provide sufficient confinement to the in-filled concrete.
- The cogged bars were subjected to unidirectional cyclic loading in tension for many cycles and behaved in a stable, reliable manner. The cyclic backbone load-slip curves are similar to the corresponding monotonic load-slip curves.
- A nonlinear finite element model was developed and validated against the experimental results for the load versus slip behaviour of the anchored bars. The anchorage model gave good predictions when compared with the experimental results. Furthermore, the ultimate capacity and failure mode correlated with experimental observations.
- A parametric study has been performed numerically to determine the influence of the tube wall thickness. The thickness of a 323.9 mm diameter tube was varied from 20 mm down to 2 mm (D/t ratio from 16 to 162). The analysis confirmed that the level of confinement provided by steel tube has very little effect on the pull-out vs. slip behaviour of single cogged bars for D/t values in this range.

References

- Abaqus (2012), Abaqus User Manual; Dassault Systems.
- ACI (2005), ACI Building Code Requirements for Structural Concrete (ACI 318-05) and Commentary (ACI 318R-05); American Concrete Institute.
- AS/NZS4671 (2001), AS/NZS4671 Steel Reinforcing Materials; Standards Australia, Sydney, Australia.
- AS1163 (1991), AS1163 Cold-formed structural steel hollow sections; Standards Australia, Sydney, Australia.
- AS3600 (2001), AS3600 Concrete structures; Standards Australia, Sydney, Australia.
- Ashadi, H. and Bouwkamp, J. (1995), "Behaviour of hybrid composite structural earthquake resistant joints", *Proceedings of the 10th European Conference on Earthquake Engineering*, Rotterdam, The Netherlands, pp. 1619-1624.
- CEN (2004), Eurocode 2: Design of Concrete Structures – Part 1-1: General Rules and Rules for Buildings; European Committee for Standardization, Brussels, Belgium.
- Eligehausen, R., Popov, E. and Bertero, V. (1983), "Local bond stress-slip relationships of deformed bars under generalized excitations", Report No. UCB/EERC 83-23; University of California, Berkeley, CA, USA.
- Haskett, M., Oehlers, D.J. and Mohamed Ali, M.S. (2008), "Local and global bond characteristics of steel reinforcing bars", *Eng. Struct.*, **30**(2), 376-383.
- Hossain, A. and Khandaker, M. (2008), "Bond characteristics of plain and deformed bars in lightweight pumice concrete", *Construct. Build. Mater.*, **22**(7), 1491-1499.
- Kamal, M.M., Safan, M.A. and Al-Gazzar, M.A. (2013), "Steel-concrete bond potentials in self-compacting concrete mixes incorporating dolomite powder", *Adv. Concrete Construct.*, **1**(4), 273-228
- Kang, T.H.K., Ha, S.S. and Choi, D.U. (2010), "Bar pullout tests and seismic tests of small-headed bars in

- beam-column joints”, *ACI Struct. J.*, **107**(1), 32-42.
- Mirza, O. and Uy, B. (2011), “Behaviour of composite beam–column flush end-plate connections subjected to low-probability, high-consequence loading”, *Eng. Struct.*, **33**(2), 647-662.
- Paulay, T. and Priestley, M. (1992), *Seismic Design of Reinforced Concrete and Masonry Buildings*, John Wiley & Sons.
- Pitrakkos, T. and Tizani, W. (2013), “Experimental behaviour of a novel anchored blind-bolt in tension”, *Eng. Struct.*, **49**, 905-919.
- Plizzari, G., Deldossi, M. and Massimo, S. (1998), “Transverse reinforcement effects on anchored deformed bars”, *Magazine of Concrete Research*, **50**(2), 161-177.
- Scott, R.H. (1996), “Intrinsic mechanisms in reinforced concrete beam-column connection behaviour”, *ACI Struct. J.*, **93**(3), 336-346.
- Seo, J., Lee, G.C., Liang, Z. and Dargush, G.F. (2014), “Configuration and size effects on bond stress-slip and failure modes of RC connections”, *J. Eng. Mec.*, **140**(11), 04014082.
- Soroushian, P. and Choi, K. (1989), “Local bond of deformed bars with different diameters in confined concrete”, *ACI Struct. J.*, **86**(2), 217-222.
- Soroushian, P., Obaseki, K., Nagi, M. and Rojas, M.C. (1988), “Pullout behaviour of hooked bars in exterior beam-column connections”, *ACI Struct. J.*, **85**(3), 269-276.
- Soroushian, P., Choi, K., Park, G. and Aslani, F. (1991), “Bond of deformed bars to concrete: Effects of confinement and strength of concrete”, *ACI Mater. J.*, **88**(3), 227-232.
- Tizani, W., Ali, A.-M., Owen, J.S. and Pitrakkos, T. (2013), “Rotational stiffness of a blind-bolted connection to concrete-filled tubes using modified hollo-bolt”, *J. Construct. Steel Res.*, **80**, 317-331.
- Yao, H., Goldsworthy, H. and Gad, E. (2008), “Experimental and numerical investigation of the tensile behavior of blind-bolted T-stub connections to concrete-filled circular columns”, *J. Struct. Eng.*, **134**(2), 198-208.

DL